Photoradiosynthesis of 68Ga-Labeled HBED-CC-Azepin-MetMAb for Immuno-PET of c-MET Receptors

Fay, Rachael ; Gut, Melanie ; Holland, Jason P

Abstract: In an alternative approach for radiotracer design, a photoactivatable HBED-CC-PEG3-ArN3 chelate was synthesized and photoconjugated to the anti-c-MET antibody MetMAb (onartuzumab). Photoconjugation gave the functionalized protein HBED-CC-azepin-MetMAb with a photochemical conversion of 18.5 ± 0.5% (n = 2) which was then radiolabeled with 68Ga3+ ions. The purified and formulated [68Ga]GaHBED-CC-azepin-MetMAb radiotracer was evaluated in vitro and in vivo. Standard stability tests and cellular binding assays confirmed that the radiotracer remained radiochemically pure and immunoreactive after photochemical conjugation. [68Ga]GaHBED-CC-azepin-MetMAb showed specific uptake in c-MET-positive MKN-45 (high-expression) and PC-3 (low/moderate expression) tumors with tumor-associated activities at 6 h post-administration of 10.33 ± 1.27 (n = 5) and 3.88 ± 1.27 (n = 3) %ID/g, respectively. In competitive blocking experiments, MKN-45 tumor uptake was reduced by approximately 55% (P-value <0.001 compared with nonblocked experiments) confirming specific radiotracer binding to c-MET in vivo. Radiochemical, cellular, and in vivo experiments confirmed that the photoradiochemical approach is a viable tool to synthesize new radiotracers for immuno-PET.

DOI: https://doi.org/10.1021/acs.bioconjchem.9b00342

Photoradiosynthesis of ^{68}Ga-labelled HBED-CC-azepin-MetMAb for immuno-PET of c-MET receptors

Rachael Fay, Melanie Gut and Jason P. Holland*

University of Zurich, Department of Chemistry, Winterthurerstrasse 190, CH-8057, Zurich, Switzerland

*** Corresponding Author:**

Prof. Dr Jason P. Holland

Tel: +41.44.63.53.990

E-mail: jason.holland@chem.uzh.ch

Website: www.hollandlab.org

First author:

Rachael Fay

Email: rachael.fay@chem.uzh.ch

Running Title: *Photoradiochemical labelling of MetMAb for immuno-PET imaging of c-MET receptors*

Words (Main text): 4685

Abstract

In an alternative approach for radiotracer design, a photoactivatable HBED-CC-PEG_3-ArN_3 chelate was synthesised and photoconjugated to the anti-c-MET antibody MetMAb (onartuzumab). Photoconjugation gave the functionalised protein HBED-CC-azepin-MetMAb with a photochemical conversion of 18.5±0.5% (n = 2) which was then radiolabelled with $^{68}Ga^{3+}$ ions. The purified and formulated [^{68}Ga]GaHBED-CC-azepin-MetMAb radiotracer was evaluated *in vitro* and *in vivo*. Standard stability tests and cellular binding assays confirmed that the radiotracer remained radiochemically pure and immunoreactive after photochemical conjugation. [^{68}Ga]GaHBED-CC-azepin-MetMAb showed specific uptake in c-MET-positive MKN-45 (high-expression) and PC-3 (low/moderate expression) tumours with tumour-associated activities at 6 h post-administration of 10.33±1.27 (n = 5) and 3.88±1.27 (n = 3) %ID/g, respectively. In competitive blocking experiments, MKN-45 tumour uptake was reduced by approximately 55% (P-value < 0.001 compared with non-blocked experiments) confirming specific radiotracer binding to c-MET *in vivo*. Radiochemical, cellular and *in vivo* experiments confirmed that the photoradiochemical approach is a viable tool to synthesise new radiotracers for immuno-PET.

Keywords: ^{68}Ga, photoradiochemistry, immuno-PET, hepatocyte growth factor receptor (c-MET), MetMAb

Introduction

Antibody-based PET imaging (immuno-PET) is an invaluable tool for cancer diagnosis and further monitoring of the efficacy and patient response to chemotherapy. Accessing radiolabeled antibodies in a clinical setting relies on traditional bioconjugation methods which usually involve protein ligation at lysine or cysteine residues using amide, thioester and maleimide thiol coupling reactions. Until recently, only a handful of studies had investigated the use of photochemical conjugation methods in radiotracer synthesis.[1–10][11] In 2019, our group demonstrated that photochemical activation of chelates bearing aryl azide groups gave efficient conjugation and radiolabelling to monoclonal antibodies forming viable radiotracers for immuno-PET.[12,13] In this work, we sought to extend this photoradiochemical approach to engineered immunoglobulins by conjugating the c-MET targeting antibody MetMAb with the novel acyclic photoactive chelate HBED-CC-PEG_3-ArN_3. We report the synthesis of HBED-CC-PEG_3-ArN_3 and its applications in rapid and efficient photochemical bioconjugation. The HBED-CC-azepin-MetMAb conjugate was radiolabeled with ^{68}Ga to produce an immuno-PET radiotracer which was investigated *in vitro* and *in vivo*.

Human hepatocyte growth-factor receptor (c-MET) is a receptor tyrosine kinase which is expressed on the surface of many epithelial cells and belongs to the MET family.[14] Hepatocyte growth factor (HGF; also known as scatter factor [SF]) is the only known natural ligand for c-MET.[15] Binding of active HGF to c-MET results in receptor dimerisation and internalisation which induces cell signalling.[15] The c-MET signalling pathway is dysregulated in a number of human cancers including gastric, breast, lung, ovarian and pancreatic cancer.[16] Overexpression and amplification of the c-MET gene induces signaling cascades that influence tumour cell proliferation *via* the P13K/AKT and Ras/MAPK pathways.[14] Currently, MET inhibitors and anti-

MET antibodies show some promise in the clinical treatment of MET associated cancers but such agents are yet to receive regulatory approval.[17] Molecular imaging of c-MET expression has the potential to support the clinical evaluation of MET-targeted therapies by assisting in patient selection and in monitoring drug efficacy.[18–20]

MetMAb (onartuzumab, Genentech Inc., South San Francisco, CA) contains a humanized one-armed monovalent anti-MET antibody designed to bind the extracellular domain of c-MET and thereby block activation by HGF.[21,22] MetMAb has been investigated in phase III trials as a treatment for non-small-cell lung cancer (NSCLC).[21] The antibody component, onartuzumab, was constructed using "knobs into holes" technology and a one-armed design was employed to prevent the dimerisation of the c-MET receptor upon binding, thereby avoiding the activation of signal transduction.[19,21]

Recent work using onartuzumab coupled to ^{89}Zr and ^{76}Br radionuclides *via* standard isothiocyanate conjugation techniques or direct bromination of tyrosine residues respectively illustrated the utility of MetMAb as an immuno-PET agent for imaging c-MET.[19,20] These initial studies indicate the ability of a MetMAb radiotracer to distinguish between tumours with high (MKN-45) and low (U87-MG) c-MET expression.[19] Prior success in using MetMAb to develop radiotracers for immuno-PET confirms that this modified antibody is a suitable benchmark for evaluating if photoradiochemistry can be applied to engineered proteins.

Results and Discussion

Synthesis of a photoactive chelate for coordinating $^{68}Ga^{3+}$ ions

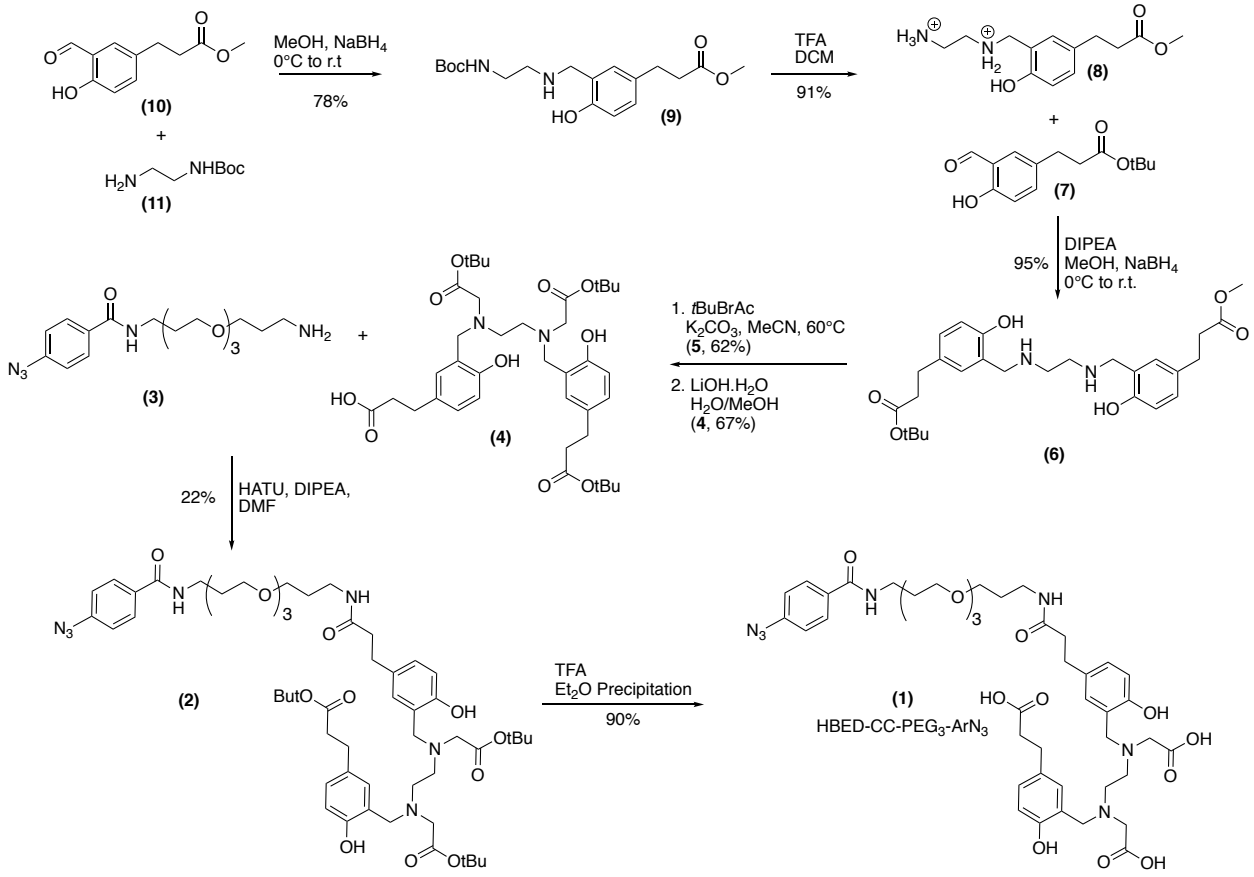

Scheme 1. Synthetic route toward HBED-CC-PEG$_3$-ArN$_3$ (**1**).

The synthesis of HBED-CC-PEG$_3$-ArN$_3$ (**1**) is depicted in Scheme 1. Full synthetic details and characterisation data are reported in the supplementary information (Supporting Figures 1 – 2, and 9 – 18). Briefly, the protected ester, HBED-CC(O*t*Bu)$_3$, (**4**) was synthesised in 5 linear steps from compounds **10** and **11** in a procedure adapted from Zha *et al.*[23] Synthesis of the NH$_2$-PEG$_3$-ArN$_3$ (**3**) was as previously described.[12] The protected chelate (**4**) was coupled to the aryl azide (**3**) *via* standard amide coupling. *Tert*-butyl protecting groups were cleaved using trifluoroacetic acid to yield HBED-CC-PEG$_3$-ArN$_3$ (**1**) in an overall yield of 5.5%. The HBED-CC chelate is a hexa-dentate ligand that leads to highly stable complexes with $^{68}Ga^{3+}$ ions (log β = 38.5).[24] The desired

photoactive chelate (**1**) was moderately soluble in water (≈1 mM), and solubility improved (≈2.5 mM) under basic conditions.

The photoactive properties of compound **1** were investigated by the means of photochemical degradation experiments. Solutions of compound **1** were irradiated (LED intensity 50% [full power = 92 mW], 365 nm) and aliquots of the irradiated solution were analysed by HPLC at various time points (Supporting Figure 2). Experiments confirmed that compound **1** was photoactive and kinetic studies determined that under the conditions employed, photodegradation was complete in <10 min as indicated by complete consumption of starting material **1**.

Photochemical conjugation

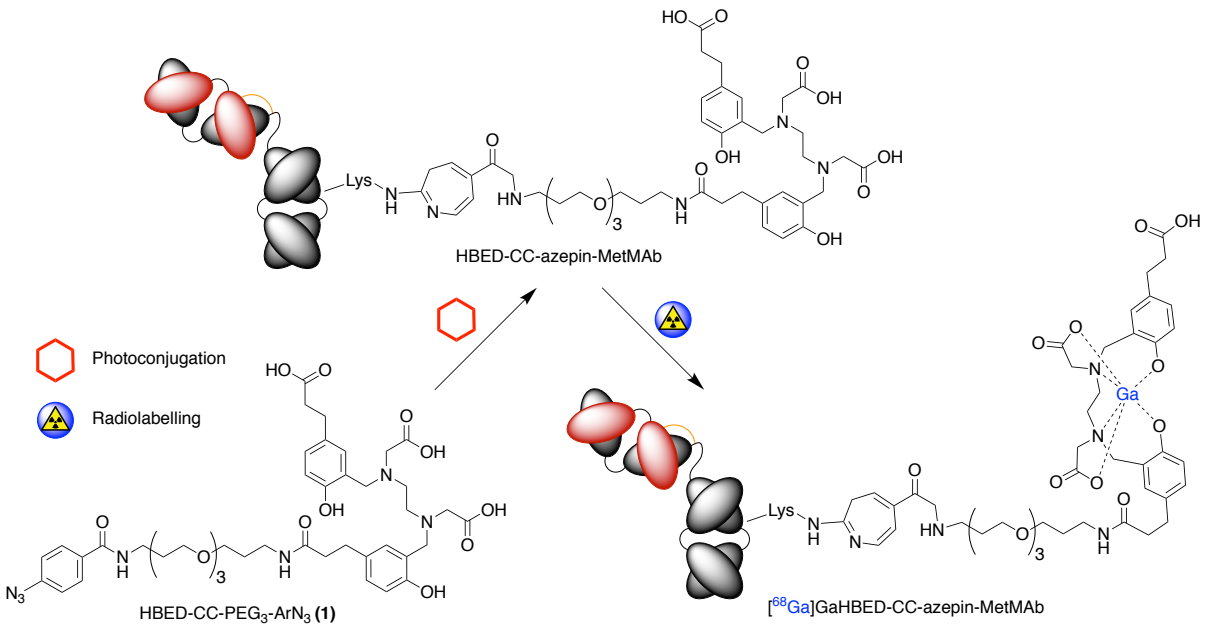

Scheme 2. Reaction scheme showing the sequential photochemical conjugation and radiolabelling to yield [^{68}Ga]GaHBED-CC-azepin-MetMAb.

The two-step photoradiochemical method is shown in Scheme 2. Previous mechanistic studies showed that nucleophilic attack by a primary amine group of a protein on the photo-induced ketenimine intermediate yields a stable covalent conjugated protein *via* formation of a 7-membered heterocyclic azepine ring.[25]

The antibody component of MetMAb was recovered in sterile saline and was incubated with a 5-fold excess of HBED-CC-PEG_3-ArN_3 (**1**) at room temperature under basic conditions at pH 8 – 9. The reaction was irradiated for 10 min. then excess chelate was removed by multiple centrifugal filtration cycles. Aliquots of the crude photochemical conjugation reactions were retained prior to purification and subsequently radiolabelled with ^{68}Ga to determine the photochemical conversion (PCC). Radiolabelled samples were analysed by radioactive-size-exclusion chromatography (radio-SEC) with a mobile phase of PBS (Gibco, pH 7.4) and decay-corrected chromatograms were integrated to determine the ratio of labelled protein to excess ^{68}Ga-complexes. Subsequent radio-SEC analysis gave a photoradiochemical conversion of 18.5±0.5 % (n = 2). If it assumed that compound **1** and the metallated [^{68}Ga]Ga(**1**) complex have equivalent photochemical initiation and conjugation efficiencies, then with an initial 5-fold excess the estimated upper-limit to the number of bound and chemically accessible chelates per antibody was 0.93±0.03. In practice, the reactivity and PCC between free chelates and metallated complexes is different. The actual chelate-to-antibody ratio in the final product is likely to be lower and depends strongly on the initial specific activity and radiochemical purity of the radionuclide source.

Liquid chromatography mass spectrometry (LCMS) analysis using time-of-flight (TOF) measurements of the photochemically conjugated MetMAb was also conducted. From these data, a shift in the mass spectrum was observed corresponding to one chelate modification (Supporting Figure 4) which corroborated the success of the photochemical conjugation process.

Photochemical conjugation experiments using MetMAb in formulation buffer (10 nmol L^{-1} histidine succinate, 106 nmol L^{-1} trehalose dihydrate, 0.02% polysorbate 20, pH 5.7) rather than pre-purified in saline were also conducted.[21] Under equivalent photochemical and radiolabelling conditions, [^{68}Ga]GaHBED-CC-azepin-MetMAb was still obtained from fully formulated samples of MetMAb but the PCC reduced to ~10%. Reduced PPC is likely due to the presence of histidine in the formulation buffer which competes with MetMAb lysine residues for nucleophilic attack on the ketenimine intermediate. Nevertheless, successful photochemical conjugation and radiolabelling direct from a formulated protein source is unprecedented and illustrates one of the potential advantages of using our photoradiochemical approach over existing methods.

Many existing bioconjugation techniques are inefficient and require a large excess of chelate due to aqueous instability of activated NHS or TFP esters.[26] Furthermore, many activated chelates are poorly soluble in aqueous conditions and require addition of organic solvents (e.g. DMSO/EtOH) which can result in degradation or precipitation of biomolecules. The photochemical approach has the advantages that the reaction is fast (~10 min.), and that the derivatised chelate is water soluble and stable as a stock solution when protected from light. The reaction is also relatively efficient, and reproducible with only 5-fold excess of chelate required to produce a bioconjugate with sufficiently high molar activity for *in vivo* experiments.

Photoradiosynthesis of [^{68}Ga]GaHBED-CC-azepin-MetMAb

[^{68}Ga][Ga(H_2O)$_6$]Cl_3(aq.) was obtained by elution of a ^{68}Ge/^{68}Ga-generator with HCl (0.1 M). All ^{68}Ga-labelling experiments were performed in acetate buffer (0.25 M, pH 4.4) at room temperature. Radio-TLC methods using a citrate eluent (pH 4) were used to follow the course of all radioactive experiments.

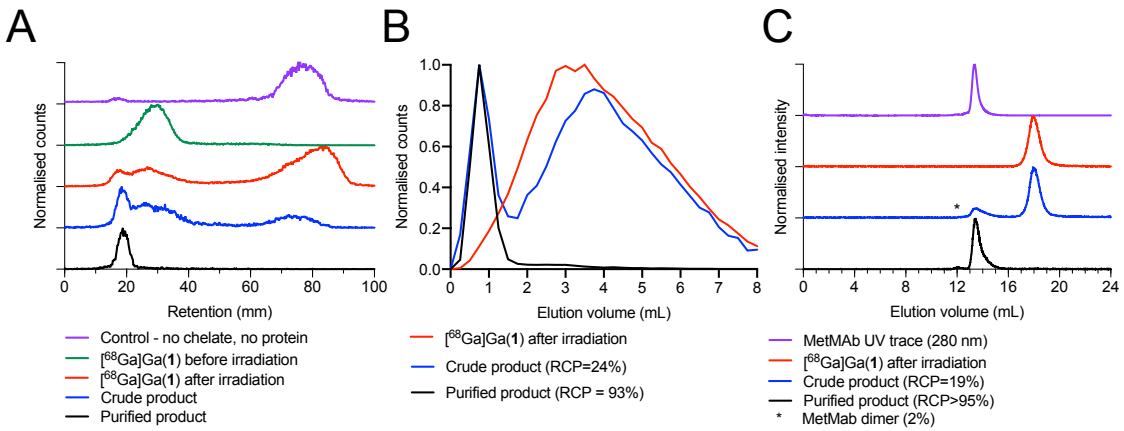

137

138 **Figure 1. A**) Radio-iTLC data for [^{68}Ga]GaHBED-CC-PEG$_3$-ArN$_3$ species, control samples, and
139 subsequent photochemical conjugation to MetMAb. **B**) PD-10 elution profiles showing the
140 analysis of the photochemical conjugation and ^{68}Ga-radiolabelling of HBED-CC-PEG$_3$-ArN$_3$ to
141 MetMAb. **C**) Electronic absorption and radio-SEC-HPLC data showing chromatograms for
142 [^{68}Ga]GaHBED-CC-azepin-MetMAb and related controls.

143

144 Figure 1 shows the radio-iTLC profiles of the control, [^{68}Ga][Ga(citrate)$_2$]$^{3-}$ (R_f = 1.0),
145 [^{68}Ga]Ga(**1**) (R_f = 0.03 – 0.32; green trace), irradiated [^{68}Ga]Ga(**1**) (red trace), the ^{68}Ga-
146 radiolabeled crude photochemical conjugation (blue trace), and the purified [^{68}Ga]GaHBED-CC-
147 azepin-MetMAb (R_f = 0.0; black trace) radiotracer in panel A. Irradiation of [^{68}Ga]Ga(**1**) results
148 in three peaks on radio-TLC, with one of these migrating to the solvent front (R_f = 1.0). This result
149 can be explained by the number of different polar species generated by irradiation of compound
150 (**1**) as shown in Supporting Figure 2. Radio-iTLC in a different eluent system (MeOH/H$_2$O 1:1)
151 showed that this peak at the solvent front was not associated with "free" ^{68}Ga^{3+} ions, which in this
152 solvent system was retained at the baseline as [^{68}Ga][Ga(OH)$_3$].

153 Two different size exclusion chromatography (SEC) methods were used to measure decay
154 corrected radiochemical purity (RCP) and yields. PD-10 SEC was used for preparative purification

prior to *in vitro* and *in vivo* experiments. PD-10 elution profiles of irradiated [^{68}Ga]Ga(**1**), the ^{68}Ga-radiolabeled crude photochemical conjugation (RCP = 24%), and the purified [^{68}Ga]GaHBED-CC-azepin-MetMAb (RCP = 93%) are shown in Figure 1B. Data confirm that a portion of the ^{68}Ga-radioactivity in the crude mixtures eluted with the high molecular weight protein fraction. However, due the overlapping elution profiles of irradiated [^{68}Ga]Ga(**1**) (red trace) and the crude ^{68}Ga-radiolabeled product (blue trace) in analytical PD-10 SEC methods, we used high performance liquid chromatography (radio-SEC-HPLC, coupled to a BioRad 650 ENrich column) to determine accurate values for the RCP. The UV-SEC (280 nm) trace of native MetMAb and the radio-SEC-HPLC traces of irradiated [^{68}Ga]Ga(**1**), the ^{68}Ga-radiolabeled crude photochemical conjugation (RCP = 19%), and the purified [^{68}Ga]GaHBED-CC-azepin-MetMAb (RCP >95%) are shown in Figure 1C.

The molar activity of [^{68}Ga]GaHBED-CC-azepin-MetMAb was estimated as 35.8±2.00 MBq nmol^{-1} (n = 8) as measured by titrations of [^{68}Ga]GaHBED-CC-azepin-MetMAb against a ^{68}Ga stock solution of known molar activity. After purification by preparative PD-10 SEC, high purity [^{68}Ga]GaHBED-CC-azepin-MetMAb was formulated in sterile PBS for *in vivo* experiments (RCP>95%, radio-SEC analysis, Figure 1C, black trace). Formulated [^{68}Ga]GaHBED-CC-azepin-MetMAb was isolated with a molar activity A_m = 22.3 MBq nmol^{-1} and an isolated decay-corrected radiochemical yield (RCY) of 55%.

Cell culture

The human prostate cancer cell line PC-3 (c-MET +ve moderate expressing, ATCC) and the human gastric cancer cell line MKN-45 (c-MET +ve high expressing, DKMZ) were used for *in vitro* and *in vivo* studies. The human prostate cancer cell line, LNCaP (c-MET -ve, ATCC) was

used as a control *in vitro* for Western blot analysis. Full cell culture methods are presented in the supporting information.

Western blot analysis

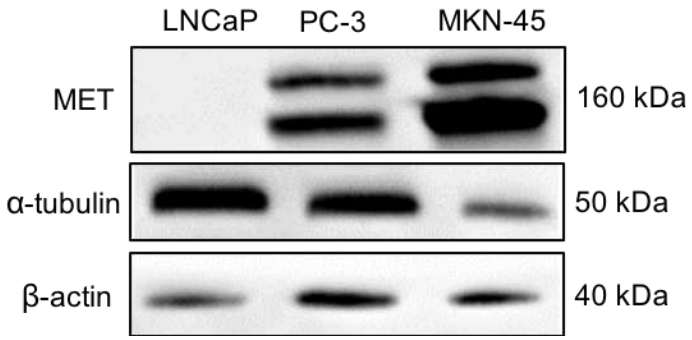

Figure 2. Western blot images showing the MET content of three cell lysates: LNCaP (negative control), PC-3 and MKN-45.

Western blot analysis of normalised protein concentration cell lysates (LNCaP, PC-3, MKN-45), shown in Figure 2, indicated that the negative control LNCaP lysate contained no c-MET, the PC-3 lysate contained a low/moderate amount of c-MET, and the MKN-45 cell lysate had a very high c-MET protein content (Figure 2). Full details of the Western blot technique are presented in the supporting information. The two bands present for MET protein correspond to precursor-MET (≈175 kDa) and mature-MET (≈145 kDa) as previously described.[27] Due to variations in the concentrations of "housekeeping" proteins between different cell lines, two loading controls were used (α-tubulin and β-actin). Although significant differences were seen in the α-tubulin bands, β-actin bands appeared consistent for the three cell lines.

Cellular Binding Studies

The immunoreactive fraction (IF) was determined *in vitro* using two different cell lines with either high (MKN-45) or low/moderate (PC-3) c-MET expression. The saturation binding plot and the corresponding Lindmo reciprocal plot for the MKN-45 line are presented in Supporting Figure 3. Standard Lindmo assays confirmed that [^{68}Ga]GaHBED-CC-azepin-MetMAb remained immunoreactive and bound specifically to both MKN-45 (IF = 57±3%) and PC-3 cells (IF = 41±2%).[28] It should be noted that the number of cells required to achieve a non-linear binding profile for the PC-3 line was three times higher ($33x10^6$) than for the MKN-45 line ($11x10^6$). The lower c-MET concentration (as observed by Western blot analysis, Figure 2) leads to slower binding kinetics, and therefore, saturation binding is not reached under the experimental conditions which explains the relatively lower immunoreactive fraction. Full protocols for cellular binding studies are given in the supporting information.

Irradiation of a biomolecule with UV light is potentially detrimental to its biological activity. Therefore, experiments to determine if irradiation at 365 nm affected the immunoreactivity of a bioconjugate were conducted. For these experiments we employed DFO-NCS-MetMAb as a model conjugate that was produced *via* a conventional protein ligation route. *p*-NCS-Bz-DFO (CheMatech) was coupled to MetMAb using standard thiourea chemistry.[29] Aliquots of the purified conjugate were irradiated with 365 nm light at 100% LED intensity for 10, 30, or 60 min. Each sample was radiolabeled with ^{68}Ga and incubated with a fixed number of cells (5×10^6). The cellular bound fraction of radioactivity was determined for each sample using a similar method as for cell binding studies. Measurements for specific binding were performed in triplicate. The resulting cell bound activity (including a measure of non-specific binding) is shown in Figure 3. Furthermore, no discernable difference was observed between the measured immunoreactive fractions recorded for the radiotracer produced by the photoradiochemical process

(IF = 57±3%, Supporting Figure 3) and that produced from the conventional conjugation route (63±5%, SF3). No statistically significant difference (n = 3, P-value > 0.1) was found between the different aliquots, indicating that irradiation at 365 nm does not affect the immunoreactivity of the MetMAb bioconjugate. It should still be considered that biomolecules do not always behave analogously, and therefore, stability of proteins towards irradiation at 365 nm should be assessed on an individual case basis.

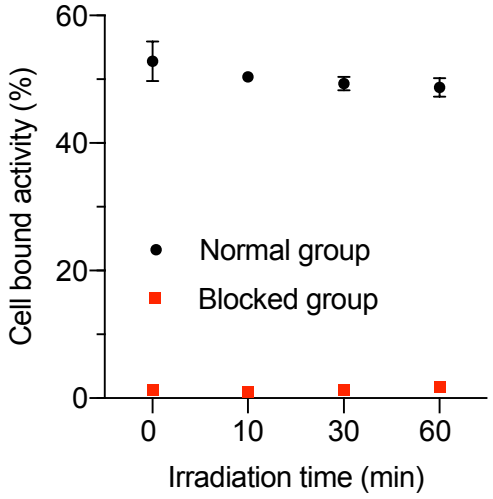

Figure 3. Plot showing the cell-associated fraction of [^{68}Ga]GaDFO-NCS-MetMAb after irradiation at 365 nm for different times.

Serum stability

The stability of [^{68}Ga]GaHBED-CC-azepin-MetMAb with respect to loss of radioactivity from the protein fraction or a change in RCP was investigated by incubation of the radiotracer in human serum albumin (HSA, Sigma Aldrich) at 37 °C. Stability studies (n = 2) were analysed using radio-SEC and showed that only a small amount of radioactivity (< 5%) was lost from the antibody over the course of 3 h (Figure 4~~A~~).

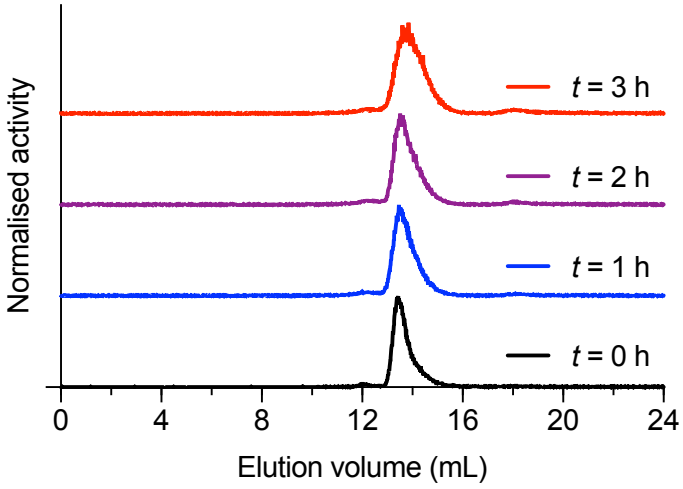

Figure 4. Stability data showing~~: A)~~ radio-SEC chromatograms of [^{68}Ga]GaHBED-CC-azepin-MetMAb incubated in HSA over 3 h at 37 °C.

Small animal PET Imaging

PET imaging was conducted in groups of mice bearing either MKN-45 (n = 5) or PC-3 (n = 3) tumours between 4 – 6 h post-administration of [^{68}Ga]GaHBED-CC-azepin-MetMAb. Mice were administered either a high molar activity formulation of [^{68}Ga]GaHBED-CC-azepin-MetMAb (normal group, A_m = 22.3 MBq nmol^{-1}, 8.26 – 11.33 MBq, 50 – 60 µg in 220 µL PBS) or a low molar activity formulation of [^{68}Ga]Ga HBED-CC-azepin-MetMAb (~~blocking~~ competitively blocked group, A_m = 1.26 MBq nmol^{-1}, 8.83 – 9.57 MBq, 1050 – 1060 µg [16.7 fold excess] in 240 µL PBS) *via* intravenous (i.v.) tail vein injection. Full details of the competitive blocking experiment are given in the supporting information. Shortly before imaging, mice were anaesthetised with isoflurane and static images were recorded for 10 minutes at 4, 5, and 6 h post-injection time points.

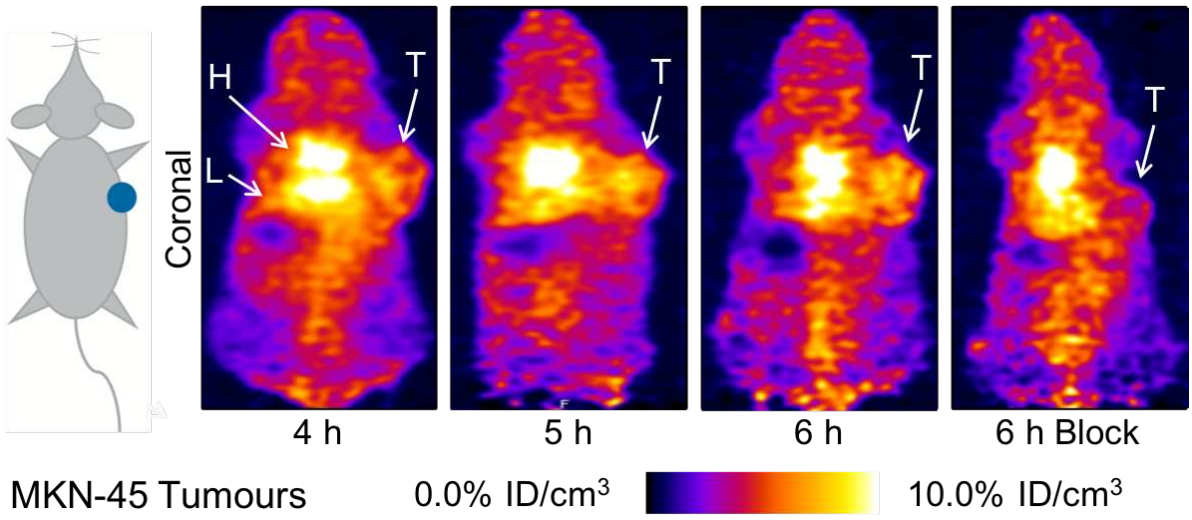

Figure 5. Longitudinal maximum intensity projection (MIP) PET images recorded in the MKN-45 model at 4, 5 and 6 h, and in the competitively blocked MKN-45 model at 6 h post-administration of [^{68}Ga]GaHBED-CC-azepin-MetMAb.

PET images recorded at 4, 5, and 6 h for the normal MKN-45 model, and an image at 6 h for the competitively blocked MKN-45 model are shown in Figure 5. Additionally, a PET image at 6 h in the PC-3 model is shown in Supporting Figure 5. In the normal MKN-45 model, tumours were easily visualised, although accumulation of radioactivity in the heart and lungs (which is representative of the circulating blood-pool activity in these in static PET imaging) contained the most activity. Immuno-PET imaging in MKN-45 and PC-3 models showed that the radiotracer remained in circulation (Heart ROI = 2.47±0.33 SUV_{mean}, 6 h, normal group, n = 5, Supporting Figure 6). Tumour-to-tissue contrast ratios are presented in Supporting Figure 7. Furthermore, images showed low clearance of the tracer through the liver (Liver ROI = 1.31±0.93 SUV_{mean}, 6 h, normal group, n = 5, Supporting Figure 6). The measured effective half-life ($t_{1/2}$(effective)) of [^{68}Ga]GaHBED-CC-azepin-MetMAb was 59.9±10.8 min (n = 3, Supporting Figure 8). This value of $t_{1/2}$(effective) is in line with the physical half-life of ^{68}Ga ($t_{1/2}$ = 67.7 min), confirming that the

radiotracer was not excreted from the body in the experimental window. Temporal PET imaging showed increased tumour uptake in MKN-45 models (Tumour ROI, SUV_{mean}= 1.39±0.14 (4 h) to 1.57±0.15 (6 h), normal group, n = 5, Supporting Figure 6). In the competitive blocking PET images, tumour uptake remained lower and constant (Tumour ROI SUV_{mean} = 1.04±0.10 (4 h) to 1.00±0.09 (6 h), blocking group, n = 5, Supporting Figure 6).

Biodistribution studies

Biodistribution studies were performed *ex vivo* at 6 h post-administration of [^{68}Ga]GaHBED-CC-azepin-MetMAb in MKN-45 and PC-3 tumour-bearing mice. Immediately after recording the final image, mice were euthanised by exsanguination under anaesthesia. Tissues were removed, washed with water, dried in air, weighed and counted using a calibrated gamma counter for accumulation of ^{68}Ga-radioactivity. Full biodistribution data sets are presented in Figure 6 and in Supporting Table S1.

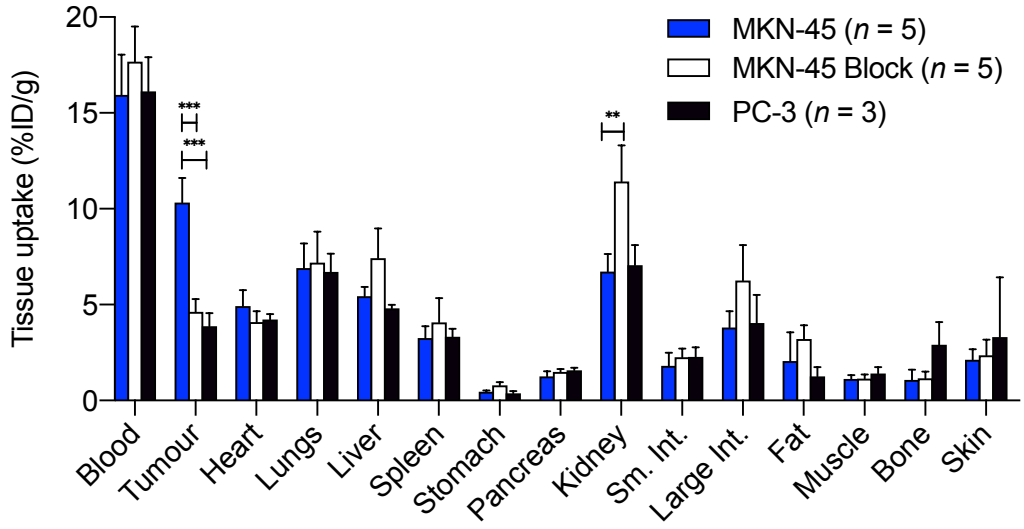

Figure 6. Biodistribution data showing the accumulation of [^{68}Ga]GaHBED-CC-azepin-MetMAb radioactivity in different tissues at 6 h post-administration in mice bearing either MKN-45 or PC-3 tumours.

Accumulation of radioactivity in the more highly expressing c-MET positive MKN-45 tumours was 10.33±1.27 %ID/g (n = 5). This value reduced to 3.88±0.68 %ID/g (n = 3, P-value < 0.001) in moderately c-MET expressing PC-3 tumours. Furthermore, the blocking study illustrated that accumulation of [^{68}Ga]GaHBED-CC-azepin-MetMAb in MKN-45 tumours could be reduced by ~55% to 4.62 ± 0.67 %ID/g (n = 5, P-value < 0.001) by co-administration of the radiotracer with higher concentrations of non-radiolabelled MetMAb. Hence, the blocking study confirmed the specific targeting of c-MET by [^{68}Ga]GaHBED-CC-azepin-MetMAb *in vivo*. Immuno-PET imaging and subsequent biodistribution studies of moderately c-MET expressing tumours (PC-3) as a control model resulted in only low accumulation (3.88 ± 0.68 ID/g) in tumour tissues. The observed low tumour uptake in the PC-3 model substantiates the results of earlier cell binding studies and provides further support that the PC-3 model has an insufficient c-MET concentration for optimal visualisation by immuno-PET using a radiotracer based on MetMAb.

We note that the combination of the short-lived ^{68}Ga radionuclide with higher molecular weight protein is clearly sub-optimal. Nevertheless, the PET and biodistribution data demonstrate that it is possible to image tumours that express high levels of c-MET with [^{68}Ga]GaHBED-CC-azepin-MetMAb at early time points. Our experiments confirm that the photoradiosynthesis approach can produce a viable radiotracer using engineered proteins that are smaller than native IgG antibodies. Experiments are underway to expanding the scope of photoradiochemistry using different chelates that facilitate labelling with radionuclides such as ^{64}Cu, ^{89}Zr, ^{90}Y, ^{177}Lu and ^{225}Ac etc. Furthermore, it is possible that the HBED-CC-azepin-MetMAb conjugate could be labelled with the longer-lived radionuclide ^{67}Ga ($t_{1/2}$ = 78.3 h) and investigated as a single-photon emission computed tomography (SPECT) imaging agent or for radioimmunotherapy (RIT).[30,31] The HBED

ligand is also known to complex $^{111}In^{3+}$ ($t_{1/2}$ = 67.3 h, log β = 39.66) for similar applications in SPECT and RIT. The side chain modification of HBED-CC-PEG_3-ArN_3 is unlikely to affect coordination to $^{111}In^{3+}$ ions.[32] The longer half-lives of the proposed tracers, [^{67}Ga]GaHBED-CC-azepin-MetMAb and [^{111}In]InHBED-CC-azepin-MetMAb, could allow greater tumour to tissue contrast ratios to be obtained by imaging at later time points.

Conclusions

The synthesis of photoactivatable HBED-CC-PEG_3-ArN_3 allowed rapid and efficient conjugation to MetMAb. Stability studies *in vitro* and *in vivo* demonstrated the viability and selectivity of [^{68}Ga]GaHBED-CC-azepin-MetMab as an immuno-PET radiotracer and confirmed that photoradiosynthesis can be applied with engineered proteins with molecular weights lower than native immunoglobulins. Immuno-PET with [^{68}Ga]GaHBED-CC-azepin-MetMAb successfully delineated tumours expressing high levels of c-MET (MKN-45, 10.33 ± 1.27 %ID/g, n = 5) and blocking studies confirmed the specificity of the tumor-associated activity. Overall, these data suggest that the combination of photochemistry and radiochemistry is a viable strategy in the design of radiotracers for immuno-PET.

Acknowledgements

JPH thanks the Swiss National Science Foundation (SNSF Professorship PP00P2_163683), the Swiss Cancer League (Krebsliga Schweiz; KLS-4257-08-2017), and the University of Zurich (UZH) for financial support. This project has received funding from the European Union's Horizon 2020 research and innovation programme / from the European

Research Council under the Grant Agreement No 676904, ERC-StG-2015, NanoSCAN. We thank all members of the Radiochemistry and Imaging Science group at UZH for helpful discussions.

Supporting Information

Supporting information is available and contains full details on the synthesis, radiochemistry, cellular assays and *in vivo* experiments.

References

(1) Hashizume, K.; Hashimoto, N.; Miyake, Y. Synthesis of Positron Labeled Photoactive Compounds: 18F Labeled Aryl Azides for Positron Labeling of Biochemical Molecules. *J. Org. Chem.* **1995**, 6680–6681.

(2) Nishikawa, M; Nakano, T.; Okabe, T.; Hamaguchi, N.; Yamasaki, Y.; Takakura, Y.; Yamashita, F.; and; Hashida, M. Residualizing Indium-111-Radiolabel for Plasmid DNA and Its Application to Tissue Distribution Study. *Bioconjug. Chem.* **2003**, 955–961.

(3) Stalteri, M. A.; Mather, S. J. Technetium-99m Labelling of the Anti-Tumour Antibody PR1A3 by Photoactivation. *Eur. J. Nucl. Med.* **1996**, 178–187.

(4) Sykes, T. R.; Woo, T. K.; Baum, R. P.; Qi, P.; Noujaim, A. A. Direct Labeling of Monoclonal Antibodies with Technetium-99m by Photoactivation. *J. Nucl. Med.* **1995**, 1913–1922.

(5) Sykes, T. R.; Somayaji, V. V; Bier, S.; Woo, T. K.; Kwok, C. S.; Snieckus, V.; Noujaim, A. A. Radiolabeling of Monoclonal Antibody B43.13 with Rhenium-188 for Immunoradiotherapy. *Appl. Radiat. Isot.* **1997**, 899–906.

(6) Grünberg, J.; Novak-Hofer, I.; Honer, M.; Zimmermann, K.; Knogler, K.; Bläuenstein, P.; Ametamey, S.; Maecke, H.R.; and Schubiger, P.A. In Vivo Evaluation Of 177Lu- and 67/64Cu-Labeled Recombinant Fragments of Antibody ChCE7 for Radioimmunotherapy and PET Imaging of L1-CAM-Positive Tumors. *Clin. Cancer Res.* **2005**, 5112–5120.

(7) Wester, H. J.; Hamacher, K.; Stöcklin, G. A. Comparative Study of N.C.A. Fluorine-18 Labeling of Proteins via Acylation and Photochemical Conjugation. *Nucl. Med. Biol.* **1996**, 365–372.

(8) Lange, C. W.; Vanbrocklin, H. F.; Taylor, S. E.; Taylor, S. E. Photoconjugation of 3-Azido-5-Nitrobenzyl-[18 F]Fluoride to an Oligonucleotide Aptamer. *J. Label. Compd. Radiopharm. J Label Compd Radiopharm* **2002**, 257–268.

(9) Pandurangi, R.S.; Karra, S.R.; Katti, K.V. ; Kuntz, R.R. and Volkert, W.A. Chemistry of Bifunctional Photoprobes. 1. Perfluoroaryl Azido Functionalized Phosphorus Hydrazides

as Novel Photoreactive Heterobifunctional Chelating Agents: High Efficiency Nitrene Insertion on Model Solvents and Proteins. *J. Org. Chem.* **1997**, 2798–2807.

(10) Pandurangi, R.S.; Lusiak, P.; Kuntz, R.R.; Volkert, W.A. ; Rogowski, J. and Platz, M.S. Chemistry of Bifunctional Photoprobes.1 3. Correlation between the Efficiency of CH Insertion by Photolabile Chelating Agents and Lifetimes of Singlet Nitrenes by Flash Photolysis: First Example of Photochemical Attachment of 99mTc−Complex with Human Serum Albumin. *J. Org. Chem.* **1998**, 9019–9030.

(11) Rajagopalan, R., Kuntz, R.R.; Sharma, U.; Volkert, W.A. and Pandurangi, R.S. Chemistry of Bifunctional Photoprobes. 6. Synthesis and Characterization of High Specific Activity Metalated Photochemical Probes: Development of Novel Rhenium Photoconjugates of Human Serum Albumin and Fab Fragments. *J. Org. Chem.* **2002**, 6748–6757.

(12) Patra, M.; Eichenberger, L. S.; Fischer, G.; Holland, J. P. Frontispiece: Photochemical Conjugation and One-Pot Radiolabelling of Antibodies for Immuno-PET. *Angew. Chemie Int. Ed.* **2019**, 1928–1933.

(13) Eichenberger, L. S.; Patra, M.; Holland, J. P. Photoactive Chelates for Radiolabelling Proteins. *Chem. Comm.* **2019**, 2257–2260

(14) Zhang, Y.; Xia, M.; Jin, K.; Wang, S.; Wei, H.; Fan, C.; Wu, Y.; Li, X.; Li, X.; Li, G.; et al. Function of the C-Met Receptor Tyrosine Kinase in Carcinogenesis and Associated Therapeutic Opportunities. *Mol. Cancer* **2018**, 1–14.

(15) Kim, K.-H.; Kim, H. Progress of Antibody-Based Inhibitors of the HGF–CMET Axis in Cancer Therapy. *Exp. Mol. Med.* **2017**, 307.

(16) Peruzzi, B.; Bottaro, D. P. Targeting the C-Met Signaling Pathway in Cancer. *Clin. Cancer Res.* **2006**, 3657–3660.

(17) Zhang, Y.; Du, Z.; Zhang, M. Biomarker Development in MET-Targeted Therapy. *Oncotarget* **2016**, 37370–37389.

(18) Han, Z.; Xiao, Y.; Wang, K.; Yan, J.; Xiao, Z.; Fang, F.; Jin, Z.; Liu, Y.; Sun, X.; Shen, B. Development of a SPECT Tracer to Image C-Met Expression in a Xenograft Model of Non–Small Cell Lung Cancer. *J. Nucl. Med.* **2018**, 1686–1691.

(19) Jagoda, E. M.; Lang, L.; Bhadrasetty, V.; Histed, S.; Kramer-marek, G.; Mena, E.; Rosenblum, L.; Marik, J.; Merchant, M.; Szajek, L.; et al. Immuno-PET Imaging of the Hepatocyte Growth Factor Receptor Met Using the One-Armed Antibody Onartuzumab (MetMAb). *J Nucl Med* **2012**, 1592–1600.

(20) Pool, M.; Terwisscha van Scheltinga, A. G. T.; Kol, A.; Giesen, D.; de Vries, E. G. E.; Lub-de Hooge, M. N. 89Zr-Onartuzumab PET Imaging of c-MET Receptor Dynamics. *Eur. J. Nucl. Med. Mol. Imaging* **2017**, 1328–1336.

(21) Xiang, H.; Bender, B. C.; Reyes, A. E.; Merchant, M.; Jumbe, N. L. “shasha”; Romero, M.; Davancaze, T.; Nijem, I.; Mai, E.; Young, J.; et al. Onartuzumab (MetMAb): Using Nonclinical Pharmacokinetic and Concentration-Effect Data to Support Clinical

Development. *Clin. Cancer Res.* **2013**, 5068–5078.

(22) Spigel, D. R.; Edelman, M. J.; O'Byrne, K.; Paz-Ares, L.; Mocci, S.; Phan, S.; Shames, D. S.; Smith, D.; Yu, W.; Paton, V. E.; et al. Results From the Phase III Randomized Trial of Onartuzumab Plus Erlotinib Versus Erlotinib in Previously Treated Stage IIIB or IV Non-Small-Cell Lung Cancer: METLung. *J. Clin. Oncol.* **2017**, 412–420.

(23) Zha, Z.; Song, J.; Choi, S. R.; Wu, Z.; Ploessl, K.; Smith, M.; Kung, H. ^{68} Ga-Bivalent Polypegylated Styrylpyridine Conjugates for Imaging Aβ Plaques in Cerebral Amyloid Angiopathy. *Bioconjug. Chem.* **2016**, 1314–1323.

(24) Tsionou, M. I.; Knapp, C. E.; Foley, C. A.; Munteanu, C. R.; Cakebread, A.; Imberti, C.; Eykyn, T. R.; Young, J. D.; Paterson, B. M.; Blower, P. J.; et al. Comparison of Macrocyclic and Acyclic Chelators for Gallium-68 Radiolabelling. *RSC Adv.* **2017**, 49586–49599.

(25) Voskresenska, V.; Wilson, R. M.; Panov, M.; Tarnovsky, A. N.; Krause, J. A.; Vyas, S.; Winter, A. H.; Hadad, C. M. Photoaffinity Labeling via Nitrenium Ion Chemistry: Protonation of the Nitrene Derived from 4-Amino-3-Nitrophenyl Azide to Afford Reactive Nitrenium Ion Pairs. *J. Am. Chem. Soc.* **2009**, 11535–11547.

(26) Lockett, M. R.; Phillips, M. F.; Jarecki, J. L.; Peelen, D.; Smith, L. M. A Tetrafluorophenyl Activated Ester Self-Assembled Monolayer for the Immobilization of Amine-Modified Oligonucleotides. *Langmuir* **2008**, 69–75.

(27) Datta, J.; Kutay, H.; Nasser, M. W.; Nuovo, G. J.; Wang, B.; Majumder, S.; Liu, C.-G.; Volinia, S.; Croce, C. M.; Schmittgen, T. D.; et al. Methylation Mediated Silencing of MicroRNA-1 Gene and Its Role in Hepatocellular Carcinogenesis. *Cancer Res.* **2008**, 5049–5058.

(28) Lindmo, T.; Boven, E.; Cuttitta, F.; Fedorko, J.; Bunn, P. A. Determination of the Immunoreactive Function of Radiolabeled Monoclonal Antibodies by Linear Extrapolation to Binding at Infinite Antigen Excess. *J. Immunol. Methods* **1984**, 77–89.

(29) Zeglis, B. M.; Lewis, J. S. The Bioconjugation and Radiosynthesis of 89Zr-DFO-Labeled Antibodies. *J. Vis. Exp.* **2015**, 52521.

(30) Young, J.D.; Abbate, V.; Imberti, C.; Meszaros, L.K.; Ma, M.T.; Terry, S.Y.; Hider, R.C.; Mullen, G.E. and Blower, P.J.Ga-THP-PSMA: A PET Imaging Agent for Prostate Cancer Offering Rapid, Room Temperature, One-Step Kit-Based Radiolabeling. *J. Nucl. Med.* **2017**, 1270–1277.

(31) Kumar, V.; Boddeti, D. K. 68Ga-Radiopharmaceuticals for PET Imaging of Infection and Inflammation. *Recent results in cancer research.* **2013**, 189–219.

(32) Mathias, C. J.; Sun, Y.; Welch, M. J.; Green, M. A.; Thomas, J. A.; Wade, K. R.; Martell, E. Targeting Radiopharmaceuticals: comparative biodistribution studies of gallium and indium complexes of multidentate ligands. *Int. J. Rad. Appl. Instrum. B.*-**1988**, 69–81.